

## IV. Department of Engineering and Technical Services

The Department of Engineering and Technical Services is involved in all kinds of work in the design, fabrication, construction and operation of experimental devices in the fields of software and hardware.

This department is composed of engineers, and their tasks fall under the following five goals:

- 1) To develop advanced and systematic engineering capabilities on the basis of basic engineering results which have been obtained thus far.
- 2) To educate excellent engineers with responsible administration.
- 3) To cultivate creative engineering abilities.
- 4) To improve the documentation of and the transfer of engineering knowledge to the next generation.
- 5) To perform tasks with a systematic responsibility.

The department consists of the following five divisions: the Fabrication Technology Division takes care of the construction of small devices and the quality control of parts for all Divisions. The Device Technology Division is responsible for LHD and LHD peripheral devices except for heating devices and diagnostic devices. The Plasma Heating Technology Division has responsibility for the ECH system, ICRF system and NBI system. The Diagnostic Technology Division develops, operates and maintains all diagnostic devices and the Control Technology Division has responsibility for the central control system, the cryogenic system, the current control system and the NIFS network. The number of staff is 46 engineers and 12 part-time workers. We take care of the development, the operation and the maintenance of LHD and the LHD peripheral devices with about 46 operators.

### 1. Fabrication Technology Division

The main work of this division is the fabrication of experimental equipment. We also take care of technical consultation and experimental parts supplies to persons concerned with the LHD experiment. In addition we handle the administrative procedures of the department.

The number of machining requests is 209 cases, and the total number of production parts is 1,102 in this FY. And for electronic engineering, these numbers are 15 and 81. The details of some activities are as follows.

#### (1) Shutter Controller

An 8ch shutter control circuit was manufactured (as shown in Fig.1) for the microwave reflectometer and the ECE (Electron Cyclotron Emission) diagnostics. This circuit prevents a high power microwave damage to the small signal microwave components. This circuit operation can be performed through the Ethernet LAN from a remote PC.



Fig. 1. Shutter controller.

#### (2) High voltage pulse amplifier

A high voltage pulse amplifier was manufactured (as shown in Fig. 2) in order to apply a 3kV bias into the terahertz pulse generator. The specifications of the amplifier are: max 150 kHz pulse frequency, +/-150V output voltage, 10mA load current. Adjusting the output voltage is done by the change of the applied voltage into the pulse switching circuit.



Fig. 2. High voltage pulse amplifier.

#### (3) Corrugated Resonator for Niigata University

We have fabricated a cylindrical cavity wall and center conductor with periodic corrugation to excite a cylindrical Bloch wave at the frequency of 170 GHz (as shown in Fig.3).

The cylindrical cavity and center conductor have 80 corrugations.

The parameters of the rectangular corrugation are a 0.3mm

width and 0.3mm depth and a periodic length of 0.5mm.

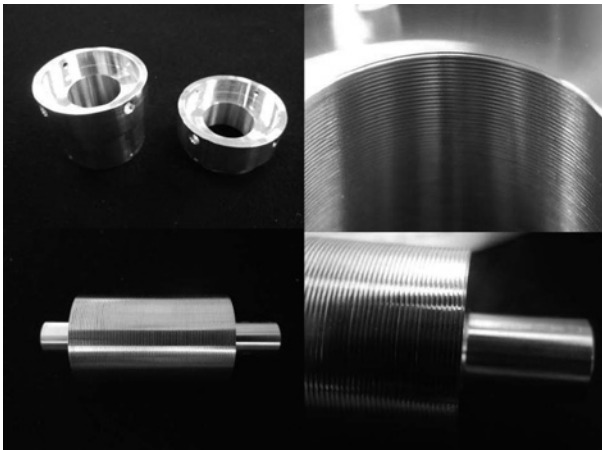


Fig. 3. Corrugated Resonator.

#### (4) Inner conductors of the new antennas for ICRF

The inner conductors (as shown as Fig. 4) of the antennas are the components of the transmission line of the ICRF. They were made for each upper or lower antenna. The inside shape is almost the same as the outside shape, nearly 6mm thickness. They are divided into 3 or 5 parts for fabrication. Each length is 635.7mm and 485.7mm. We made the complicated shape with our NC lathe. It takes 7 days to manufacture them.



Fig. 4. A picture of the inner conductors.

## 2. Device Technology Division

The Division supports the operation, the improvement and the maintenance of LHD.

### (1) Evacuation of LHD

We started to evacuate the air from the cryostat vessel for cryogenic components on July 5 and the plasma vacuum vessel on July 6. Subsequently, we checked air leaks from the maintained flanges of the plasma vacuum vessel. As a result, we found out seven leaked places and repaired them.

Next, we performed a baking operation, which involves heating with boiling water at 95 degrees Celsius, from July 19 to 23 in order to increase the sensitivity to the leaks test. After that, we checked air leaks again and no leaked places were found. Baking operation was performed again from August 1 to 8 and the glow discharge cleaning was performed from August 6, which was intended to degas from the vacuum vessel wall. During that time, we could evacuate the cryostat vessel smoothly.

The cryogenic cooling of the superconductivity coils was started on August 1. However, a refrigerant gas leak broke out from one of the voltage insulated couplings at the pipe supplying refrigerant gas to the superconductivity coils. So cooling of superconductivity coils was stopped and heated up it to room temperature by September 7.

We stopped evacuating the plasma vacuum vessel on September 4 and the cryostat vessel on September 5, and rose the both vessels pressure to atmospheric pressure in order to repair the refrigerant gas leak.

After the repair of the leak in the cryostat vessel, we started to evacuate the air from the both vessels on September 15 again. Moreover, baking operation and glow discharge cleaning was performed to degas from the vacuum vessel wall. We could evacuate the plasma vacuum vessel smoothly and it's pressure was achieved about  $2 \times 10^{-7}$  Pa on October 24.

The LHD experiment of the 16th experimental campaign began on October 17, 2012 and ran through December 6, 2012. The number of days of the plasma experimental period was 34 days in total.

During this experimental campaign, our vacuum pumping systems were able to evacuate the air from both of the vessels without trouble.

However, during the period, a large leak broke out twice at the plasma vacuum vessel. The first leak was occurred on November 15. Water (or molecular weight=18) was detected at this leak. Since the leak disappeared while we researched the cause, we failed to identify the cause of the leak. The second leak occurred on December 6 (the last day in this experimental campaign). A defect occurred in the welding area of the tile base to cool the carbon tile in the divertor leg armor at the ICRF antenna which heats the plasma. Subsequently, water which cools the armor was detected at this leak. This leak resulted in the completion of this experimental campaign.

We repaired the second leak after the experimental campaign and continued to evacuate the plasma vacuum vessel until December 13 and the cryostat vessel until December 27 (the completion of the heating the superconductivity coils to room temperature).

(2) Numerical analysis for Cryo-sorption pump in Closed Helical Divertor

In the closed helical divertor (CHD), there are the in-vessel cryo-sorption pump and the baffle structure which consists of the divertor plates and the dome structure made from the isotropic graphite, as illustrated in Fig. 5. Both the divertor plates and the dome structure are cooled by water. The divertor plasma strikes the divertor plates, and they are heated up. The surface temperature of the divertor plates is higher than 1000 degrees Celsius in the long pulse discharges with the high plasma heating power. Since the cryo-sorption pump is facing the divertor plates, it is exposed to the radiation from the high temperature area on the divertor plates. To protect the cryo-panel from the heat flux, the shield structure of the cryo-sorption pump, which consists of the water-cooled louver type shield and the Liquid Nitrogen (LN2) cooled chevron type shield, is installed.

The numerical analysis using the finite element method code (ANSYS) was carried out to evaluate the performance of the shield structure against the radiation heat flux. The simulation model is shown in Fig. 6. The divertor plates are tightly fixed by two Mo-bolts (M6) to SUS cooling pipe of 27.2 mm in diameter, through the medium of the graphite sheets of 0.1mm thickness. The water-cooled shield and the LN2 shield is made from SUS316 and copper, respectively. The LN2 shield encloses a cooling copper pipe of 19 mm in diameter. The water-cooled shield and the LN2 shield are treated with a blacking processing to prevent the reflection of light. The divertor plasma is assumed to strike the bottom edge of the divertor plates with a heat flux of 1.7MW/m<sup>2</sup> in steady state (as shown in Fig. 6). The thermal conductivity of the graphite sheet had been estimated by the comparison of the heat load test in the test facility ACT (Active Cooling Test-stand) and the temperature data by the numerical analysis of the divertor plate. The inner surface temperature of the water-cooling pipes in the divertor plates and in the water-cooled shield are 20 degrees Celsius, and that in the LN2 shield is assumed to be 80 K. Such calculations of three-dimensional heat flow with radiation, in which nearly 100,000 grid points were used, do not come cheap. A high-performance computer using parallel processing was necessary for the calculations.

Fig. 7 shows the calculated temperature distributions of the divertor plate and the shield structure. The maximum temperature difference on the LN2 shield is less than 1 degrees Celsius, even though the maximum temperature of the water cooled shield is about 300 degrees Celsius. Therefore, the thermal performance of the shield structure is

adequate to protect the cryo-panel from the heat flux from the divertor plates.

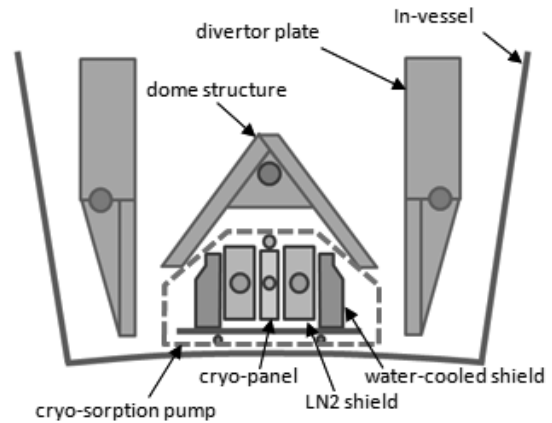


Fig. 5. Cross-sectional view of CHD

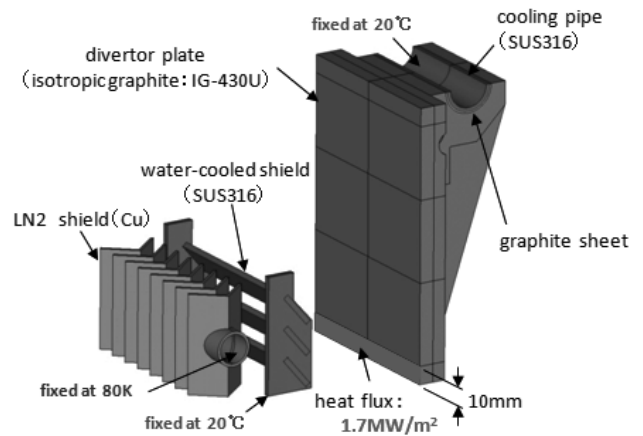


Fig. 6. Simulation model

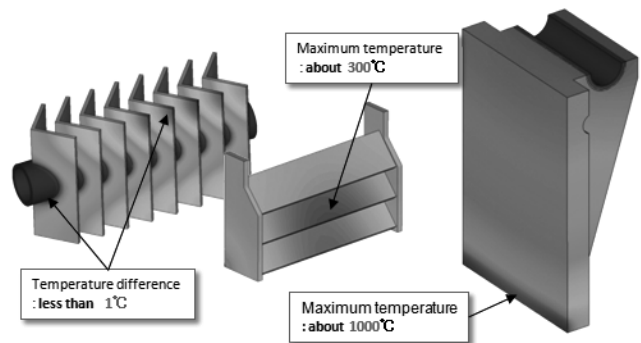


Fig. 7. Temperature distributions

(3) Cooling System for Cryo-Sorption Pumping System of Closed Helical Divertor

In the Large Helical Device, for the purpose of peripheral plasma density control by efficient particle pumping, the helical divertor region has been closed with three components (slanted divertor plates, a dome structure and target plates). And, the cryo-sorption pumping systems

have been installed under the dome structures, which have been installed at six I-port sides (2, 4, 6, 7, 8, 10-I) in the vacuum vessel. This system has been designed and developed by the members of the research staff and the department of engineering and technical service staff.

The cryo-sorption panel is cooled by heat exchange to helium gas up to about 10 K. This ultra-cold gas is derived in a cooling unit which consists of three cooling machines and six heat exchangers, and is fed in the vacuum vessel through the U-port using a helium transfer tube and is extracted from the same port. A radiation shield of the transfer tube is cooled with about 100 K helium gas which is fed from the cooling unit. Fig. 8 shows a flow diagram of the cooling system. The valve unit consists of three mass flow controllers of 100 L/min, a buffer tank of 0.32 m<sup>3</sup> and a circulation compressor for helium gas.

In the 16th experimental campaign, the pump system at only 6-I section had been put in service. This service had been carried out at the request of experimental groups. The cryo-sorption pump system had been put in service 10 times and had been worked for 395 hours within this campaign. Cooling down of cryo-sorption panels had been started from the previous night of the requested experimental day. Every night of the experimental day, the refreshment of the cryo-sorption panels had been carried out by warming up the panels to 80K and cooling it down it again. This service took about 2 hours, which had been operated by the technical staff.

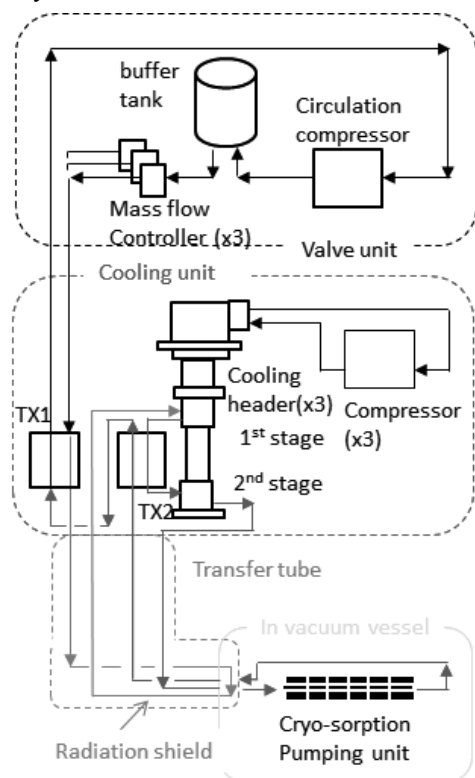


Fig. 8. Flow diagram of the cooling system

(4) Preparation of Gas-puff control system and Setting up of Super-Sonic Gas-puff (SSGP)

A gas-puff device was tuned up for the 16th experimental campaign. Injected gasses were controlled by a control PC including a DA-board and a waveform output unit in the gas control system. One of the gas control systems was broken because of aging degradation. So, we replaced it to a new gas control system (Fig. 9).

A new SSGP was installed (Fig. 10), and an additional gas control system for the SSGP was installed, too (Fig. 11).

A waveform editor to create target waveform data were improved (Fig. 12) and, a revolving light for a H<sub>2</sub> gas detector were installed (Fig. 13).

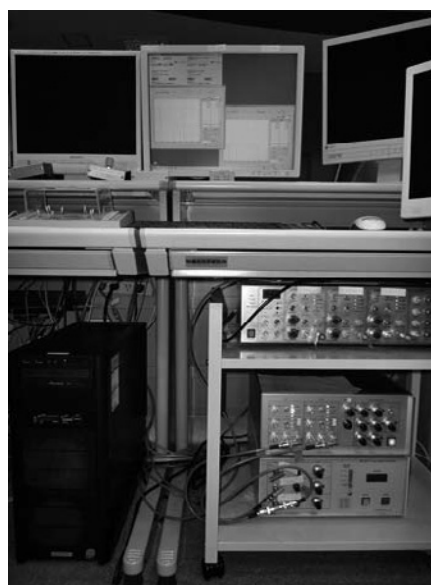


Fig. 9. New gas control system

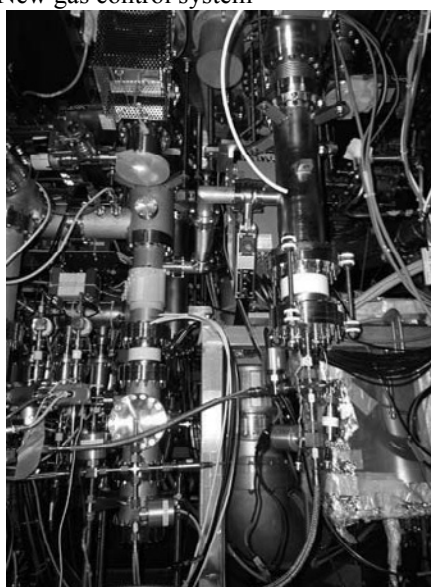


Fig. 10. Expanded SSGP



Fig. 11. Expanded gas control system

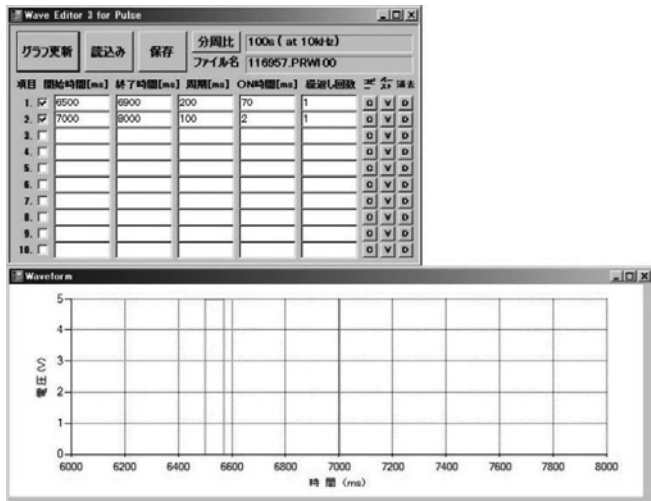


Fig. 12. Windows of improved waveform editor



Fig. 13. Installed a revolving light for a H2 detector

#### (5) Cooling Tower Renovating

This year again, we replaced the complete parts of the cooling tower since 18 years passed it was built, the scale of the replacement is one-fourth of the total. Moreover, we replaced the operational supervision equipment and reviewed the interlock conditions. For the replacement of

the equipment, we also needed to replace the monitoring tool which observe it remotely. This time, this tool was programed by ourselves. As a result, we could make the tool on the caliber of the existing one. This work resulted on an extension of the functionality.



Fig. 14. Replacement of the Cooling tower

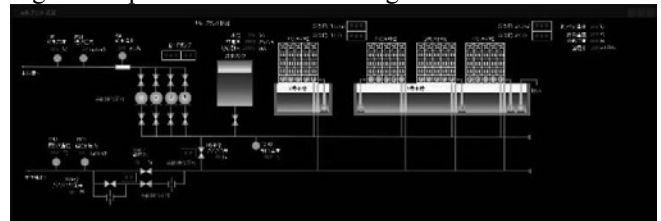


Fig. 15. Window of monitoring Tool Screen (Condition monitor display)

#### (6) Operation of X-ray killer limiter

We improved the drive control of X-ray killer limiter after the 15th experimental campaign.

As we locked the operation of the limiter manually according to the status of the experiment during the 15th experimental campaign in FY2011, we added a new function which locks the operation automatically. As a result, we could operate the limiter more safely.

The limiter was used 118 times in this experimental campaign in changing the excitation current of the coil of the LHD, and there were no serious problems.

#### (7) Operational Performance of Water Cooling System for LHD

The water cooling system which consists of three components, i.e. coolers for instruments in the mid stage and in the basement, and for ICRF heating devices, was installed in March and had been utilized for the 15th experimental campaign since July 2011. It is automatically operated from the control room. During the 16th experimental campaign, no troubles on failures were reported. Fig.16 shows a control panel of the cooling system for the instruments on the mid stage.

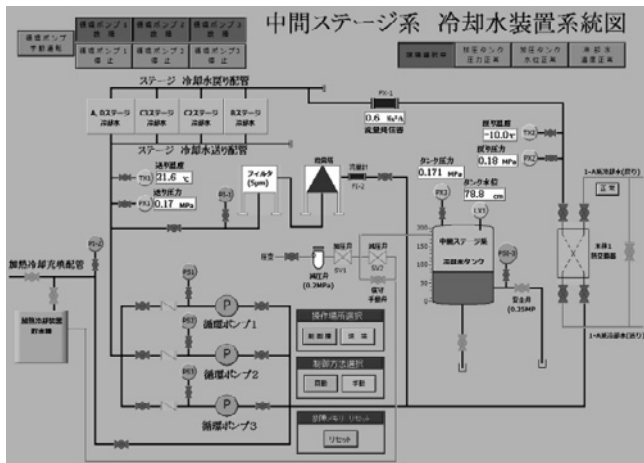


Fig. 16. Control panel of the cooling system for the instruments on the mid stage.

### (8) Maintenance of Outdoor Exhaust Pipe

We installed an outdoor exhaust pipe in the LHD hall (see Fig. 17). The purpose of this pipe is to exhaust gas from the diagnostics during a maintenance period, to decrease the quantity of dust and air in the vacuum vessel which is released to the LHD hall.

We can ventilate the vacuum vessel by connecting a vacuum vessel port to this outdoor exhaust pipe during the LHD maintenance period, discharging it to the outdoors, without releasing the ventilated air to the LHD hall. And, we can adjust the pressure in the vacuum vessel to negative pressure, which prevents the dust in the vacuum vessel from dispersing to the LHD hall. Moreover, we can respond to the individual pumping of the diagnostics in a maintenance period by installing angle valves in the outdoor exhaust pipe.

The total pipe length was about 40m. We could check that the leakage rate of the pipe was less than  $1e-8\text{Pam}^3/\text{s}$  by the leak test.

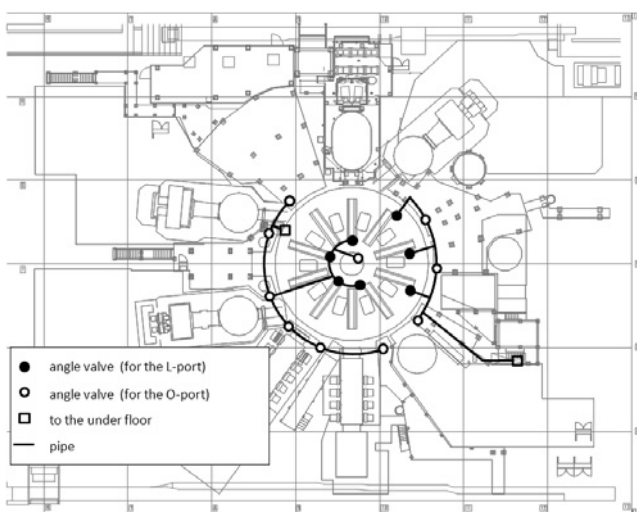


Fig. 17. The top view of the outdoor exhaust pipe in LHD

## 3. Plasma Heating Technology Division

The main tasks of this division are the operation and the maintenance of plasma heating devices and common facilities. We have also performed technical support for the improvement, the development and new installation of these heating devices.

Before this experimental campaign, one more additional 1MW/5sec output gyrotron at 154GHz was installed in the place of an old damaged 84 GHz gyrotron. As the result, the simultaneous injection power exceeded 4.6MW, enabling the achievement of the high  $T_e$  of more than 13.5keV  $n_e = 1 \times 10^{19} \text{m}^{-3}$ , for example. In the CW experiment, the plasma with  $T_{e0} = 1.5 \text{keV}$  at  $n_e = 0.7 \times 10^{19} \text{m}^{-3}$  was successfully maintained for about 30min with the averaged injection power of 0.24MW. In the 16th experimental campaign, we launched ICRF using four antennas installed at 5.5U, L and 9.5U, L ports. Using ICRF power delivered from these antenna and ECH power, 0.75 MW in total, the plasma of  $T_{e0} = 2.5 \text{keV}$  with the density of  $1 \times 10^{19} \text{m}^{-3}$  was sustained for 19min. Five NBI systems have been operated stably during the campaign. Total NB injection power reached 25.7MW. The highest ion temperature of 7.34keV is achieved by fully utilizing these NBI systems. The motor generator (MG) supplied electric power to ECH in additional to NBI.

The details of these activities are as follows.

### (1) ECH

#### (a) Gyrotron Operation & LHD experiment

During the 16th experimental campaign, we could develop the total injection power level that is approximately 1MW more than the previous campaign, since the increased power was injected by a new delivered 154GHz gyrotron. We injected ECH power stably during the whole campaign without any severe troubles that require a stop of operation for several days to restart. Especially new gyrotron highly contributed to plasma production in high temperature. Fig. 18 shows the result of ECH injection to LHD in the 16th campaign.

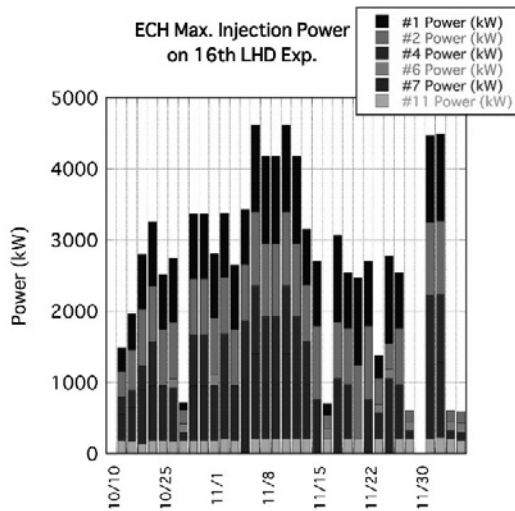


Fig. 18. History of ECH injection power during the 16<sup>th</sup> experimental campaign

(b) Improvement in Rotation Speed of Polarizer Mirror

Polarizers are used for controlling the polarization state of electron cyclotron waves and built into the power transmission lines of the LHD-ECH. A polarizer consists of a corrugated polarizer mirror and a motorized rotation stage. The polarizers are controlled using a terminal at the control room. There was a problem that the setup of the polarizer was not completed between shots. The main cause was the slow speed of the rotation stages (Max 2.5deg/s). We improved the rotation speed of one of the polarizer mirror by exchanging the motor for a high-speed one.

Fig. 19 shows the trends of torque and rotation speed when the mirror was rotated. The transmission line was evacuated. It turned out that a speed of 180deg/s was realized. The resolution of an encoder is 20 bits. The speed reduction ratio of the rotation stage is 180:1. Accuracy is sufficient. Other motors are going to be exchanged in the 2013 fiscal year.

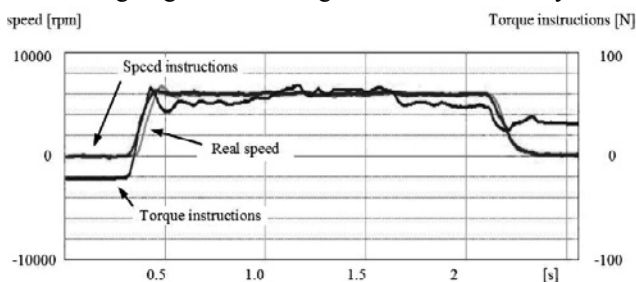


Fig. 19. Trends of motor torque and rotation speed when the mirror was rotated.

(c) Development of ECH-real-monitoring-system

To offer the information on ECH injections during and after plasma discharges, we developed an ECH-real-monitoring-system (Fig. 20). This system displays the acquired RF signals of ECH power for each

transmission line via Ethernet. Using this system, all experimental participants can share the ECH injection power and timing instantaneously and simultaneously during and after each plasma discharge.



Fig. 20. Screen shot of ECH-real-monitoring-system

(2) ICH

In the 16th experimental campaign, we carried out the LHD experiment with two HAS antennas installed at the 3.5U&L port and two Poloidal Array Antennas at the 7.5U&L port of the LHD. We used six oscillators in the experiments. The oscillators of #1 - #4 were connected to the 3.5U&L antenna and we selected two of those oscillators by the experiment frequency (38.47 MHz or 77.0 MHz). The oscillators of #5 and #6 were connected to the 7.5U&L antenna. The total injection power with the four antennas into the plasma reached 1.55 MW in the short pulse of 6 seconds at the experiment frequency of 38.47MHz. We were able to inject 0.2 MW for 1.0 second at the experiment frequency of 77 MHz for the first time by the 3.5L antenna. Sparks occurred in the vicinity of the 7.5U&L antenna during a steady state discharge, as the 15th experimental campaign. Therefore, we carried out a steady state discharge mainly using with the 3.5U&L antenna and consequently the injection power into the plasma reached 0.68 MW / 1136 seconds.

(a) Modification of program for high-speed interlock to stop self-oscillation

In the 15th experimental campaign, as the method of stopping self-oscillation, we took the detected signal of the self-oscillation in the PLC (Programmable Logic Controller) for control of the oscillators in the Heating Power Equipment Hall and made use of an interlock that was not used in the PLC. However, it took more than 6 seconds to stop the self-oscillation. Therefore, in fact we watched the state of the oscillation, and if we noticed the self-oscillation, we stopped it manually. So, we tried to

increase the speed for stopping of self-oscillation in the 16th experimental campaign. We newly had to add the inputs of the detected signal of the self-oscillation, the halt command, and the required checks for device condition on the program of the interlock. However, if they all are added to the program, an enormous number of wires are needed, and it increases the possibility of noise contamination. Moreover, compared with the number of wires, there was almost no space of the input unit on the PLC for control of the oscillator. Then, we used the input unit on the PLC for wave formation in the RF local control room as one part of the PLC for control of the oscillator and used a part of the existing program. Thus, we could reduce the newly added conditions. Since the detected signal of self-oscillation was output from the device in the same room as the PLC for wave formation, wiring between them was short. This was convenient for us. The command of the detection of self-oscillation was necessary to be sent from the PLC for wave formation to the PLC for control of oscillators. We connected the PLCs with the optical fiber cable in consideration of insulation between them. In the operation test using the simulated signal, this method could stop the self-oscillation much faster than manual stopping.

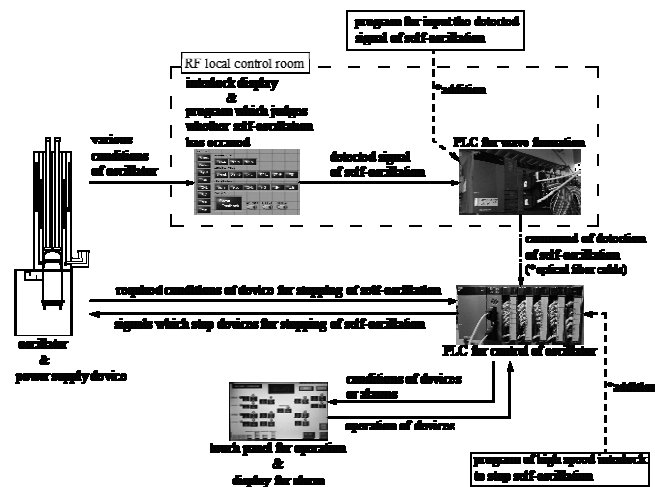


Fig. 21. Outline for stopping of self-oscillation

### (3) NBI

#### (a) Operation and maintenance of NBI in the 16th experimental campaign of LHD

Fig.22 shows the history of the total injection beam power with the negative-NBIs (BL-1, 2, and 3). About 3,700 shots of beams were injected into the LHD plasmas in this campaign. The maximum total injection power with the negative-NBIs was 14.3MW. On the other hand, with the positive-NBIs (BL-4 and 5) the total injection beam power was 11.4MW. Both the negative- and positive-NBIs were utilized for most of LHD plasma experiments with high

reliability.

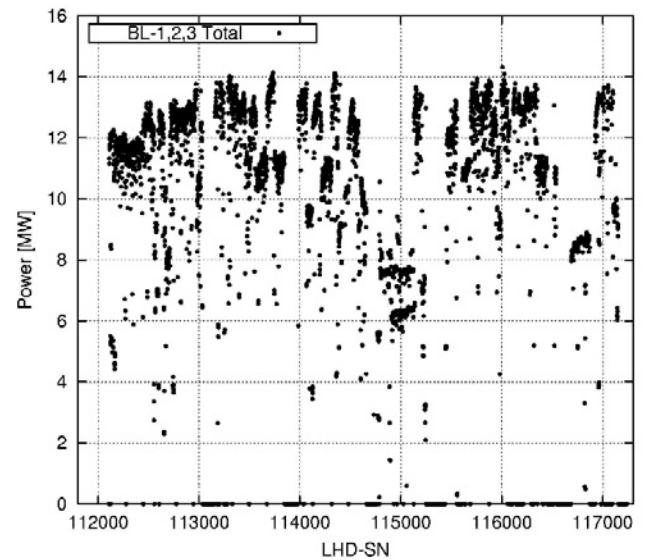


Fig. 22. History of N-NIB injection beam power

There was no big trouble in the NBI operation. Although some small troubles occurred in the control system, the power supply system, and the vacuum system, these gave no serious problem in the plasma experiments due to quick recovery. In the BL-3 ion source, there occurred a small air leak at an H2 gas inlet port. By temporary repairs, the injection performance was maintained without any reduction of the injection power.

The BL-4 will be upgraded to 60keV-9MW after the 17th experimental campaign. The engineering design is discussed for the beam-line vacuum vessel, the power supply system, and the ion sources toward the upgrade of the BL-4.

#### (b) NBI injection pattern registration system for the LHD plasma experiment

In the 16th experimental campaign, NBI injection pattern registration system was introduced as an assistance tool for the experiment leaders of LHD. Until the 15th experimental campaign, there were not any fixed formats of NBI pattern registration. Thus, it was often hard for NBI operators to understand the operation pattern required by researchers. In the new system, an electric file is distributed to the LHD experiment group via web page as a format of NBI pattern. Using this format, researchers can make the NBI operation patterns easily to input the setting conditions (injection start timing, pulse width, periods of ON/OFF of the pulse modulation, etc.). The electric file is programmed by Excel VBA and displays the result of the NBI operation pattern from the input data, which is shown in Fig. 23. This program is very useful for all LHD experiment group staff as well as NBI operators to understand the NBI operation

pattern.

In the 16th campaign, format files were uploaded to the network server and shared in LHD network. In order to solve some problems such as limited versions of Excel, we started the development of a similar system on the web service, and the NBI pattern will be able to be made and shared via a web browser in the 17th experiment campaign.

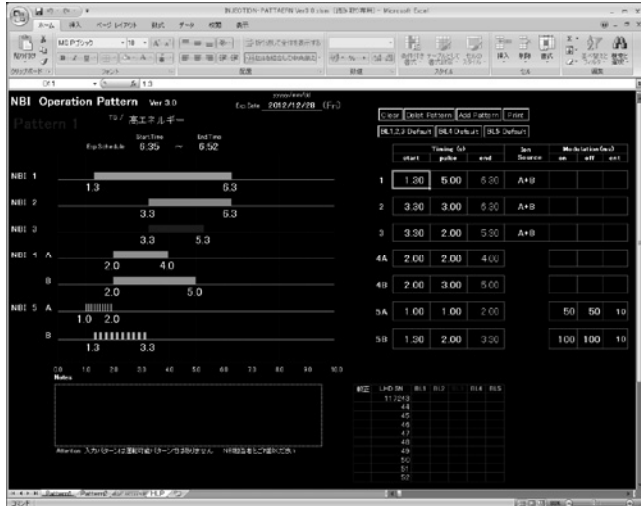


Fig. 23. Registration format programmed by Excel VBA

(c) Replacement of Infrared Camera for monitoring of Armor Tiles at Counter Wall of NB#4 Injection Port

The infrared cameras are utilized for monitoring the temperature of the armor tiles at the counter wall of the Neutral Beam (NB) injection ports. We monitor the temperature to avoid the damage of the tiles due to the excess heat loads by the beam. The infrared camera for NBI#4 was replaced from the 16th experimental campaign because it was broken.

The new infrared camera is connected to the PC through Gigabit Ethernet, and it is capable of real time 16 bit image streaming. Its image size is 320 x 240 pixels and its frame rate is 60Hz. Its temperature range is from -20 degree to 1200 degree. We only displayed its images on the monitor before the replacement. For the new camera, we have developed a new software which displays and saves the images with every injection trigger. Now, we can replay images any time. Fig. 24 shows an image of armor tiles by the infrared camera

In the 16th experimental campaign, NBI#4 injected beams about 3800 shots. The infrared camera monitored and recorded all of those shots without any trouble.

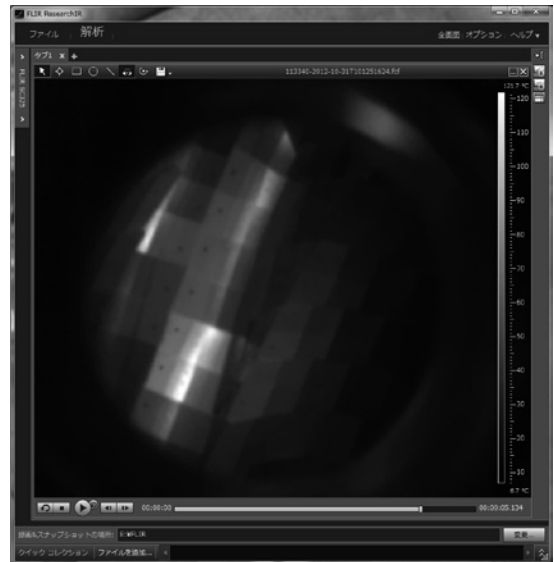


Fig. 24. Image of armor tiles by infrared camera

(4) Motor-Generator (MG)

The MG is used to supply the pulsed power to the NBI and the ECH for LHD. The MG had generated 14,651 shots in this fiscal year and 529,888 shots since its construction. The operation time was 780 hours in this fiscal year and 24,525 hours in total. Under the annual inspection in this fiscal year, the following components were checked: oil in the MG, the brushes, vacuum circuit-breakers for 6.6kV or 18kV, field circuit-breakers, contactors for the scherbius and the liquid resistor, high speed DC circuit-breaker and harmonic filter. Batteries for the control system and a diesel engine generator were replaced with new ones. Especially, the MG was rebuilt, with repaired parts that caused a water leak last year. The stator of the motor was cleaned, replaced with a new insulating spacer and painted with insulating varnish, to recover the dielectric strength.

4. Diagnostics Technology Division

This division supports utility construction and device installation work for the LHD diagnostics and the development, operation and maintenance of the diagnostic devices and of the data acquisition systems for the LHD plasma experiments. For the 16th experimental campaign, some of the diagnostics and the data acquisition systems were improved and some measuring system were operated.

In order to estimate the influence of the enhancement of the LHD in the future, we are measuring and compiling data on environmental radioactivity in the LHD building and neighboring areas. And development of the calibration system for the new interlock diagnostic systems are ongoing. In the LHD Thomson scattering diagnostics, we supported development and construction of the double pass system.

We also support operation and maintenance of FIR diagnostics, microwave reflectometer and HIBP. We carried out the preliminary vacuum leak tests on the several diagnostic devices, too. In the LHD data acquisition system, the size of whole raw data reached about 89TB in the 16th campaign. To store this huge amount of data, a cloud-based storage system is used. But considering the costs, a free software is also tested and evaluated.

Our principal tasks in this fiscal year are described in the following.

(1) Radiation Monitoring

For comparison with the future, we are measuring and compiling the data of environmental radioactivity in the LHD building and neighboring areas in the several ways (Fig. 25).

Radiation of the air in the LHD room and in the stack of the LHD building are being measured with radiation gas monitors, and the radiation of dust contained in the air is also being measured with radiation dust monitors. And, radiation of the drain water from the air-conditioning machines is also being measured. Moreover, in order to measure the extremely low level radioactive hydrogen in the stack gas, moisture contained in it is concentrated, distilled and measured with a liquid scintillation counter.

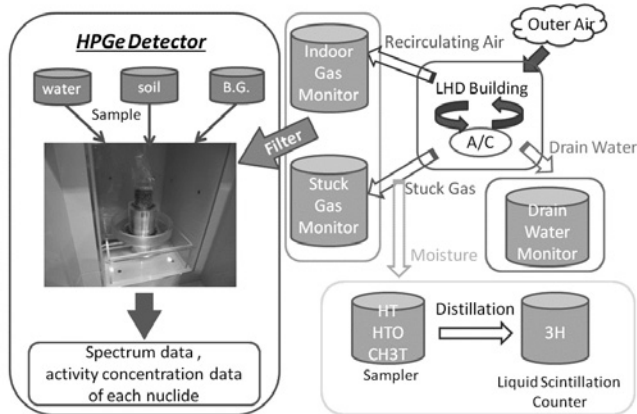


Fig. 25. Schematic view of environmental radioactivity concentration measurement system

In addition, some samples of soil or water in the site of NIFS are also measured with high-purity germanium (HPGe) detectors to investigate spectrum data and nuclide. The filters of the gas monitors are also measured with the HPGe.

(2) Interlock Diagnostic System

A movable body in the LHD vacuum vessel is used for the calibration experiment of the interlock diagnostic system (Fig. 26). It must go around the vacuum vessel at a

constant speed for a long time (>70hours). We added a voltage stabilization circuit to it and made improvements in the durability of the gear box in the motor. The running test was made out of the vacuum vessel and we confirmed it could go around constantly for 70 hours or more.

Also on assembly test within the LHD vacuum vessel was actually done, and the installation procedure was checked.

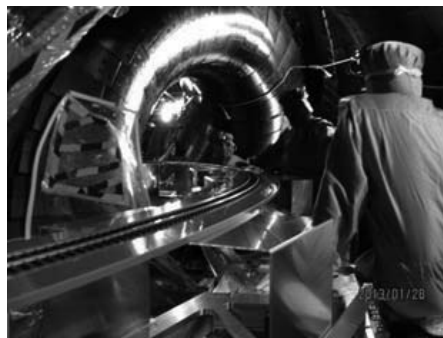


Fig. 26. Assembly test in the LHD vacuum vessel

(3) Thomson Scattering Diagnostics

In the LHD Thomson scattering diagnostics, we are constructing a double pass system by the use of a phase conjugate mirror to expand the measurable range of Te. We have successfully obtained the double pass Thomson scattering signal during the 16th campaign of the LHD experiment.

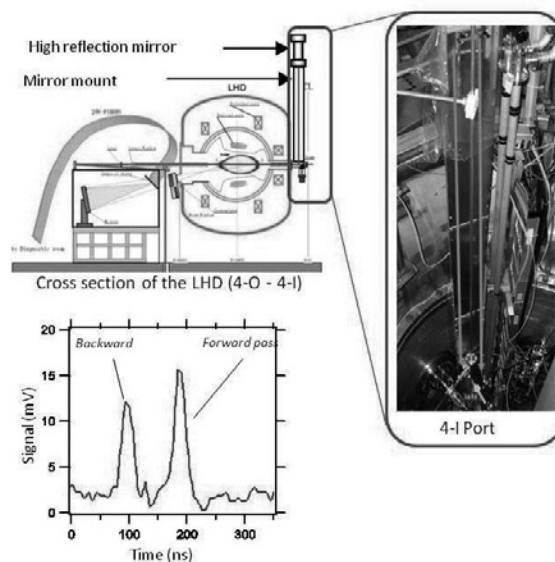


Fig. 27. The double pass system and an example of the signal

(4) Operation and Maintenance of FIR Diagnostics and Microwave Reflectometer

The operation and the maintenance (for example, high voltage power supply, vacuum pumping system, supplied gas system, phase detection circuit, dehydrater, water

cooling system etc.) were responsibly executed. Therefore in this 16th experimental campaign, in almost all shots, electron density data was taken completely. So it contributed greatly of the plasma experiment.

(5) Improvement for raising the signal strength of the HIBP

The beam section pattern detector was designed to reduce the transmission loss of a heavy ion beam.

It requires the installation of an insulated amplifier close to the detector in order to raise the detection sensitivity. So, the mount was designed to install the amplifier.

We also worked on the repair of an insulating gas (SF6) leak in the tandem accelerator.

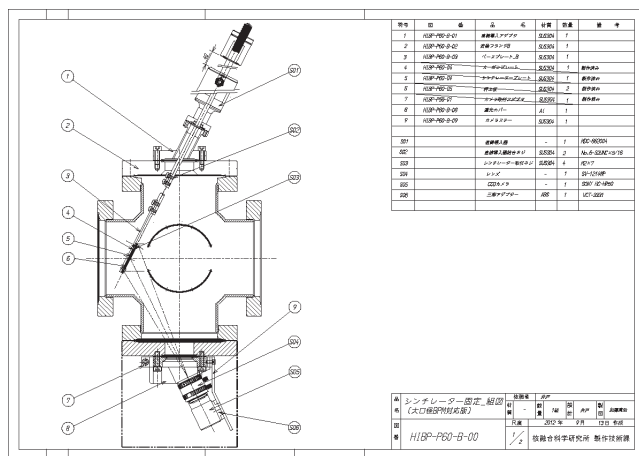


Fig. 28. Drawing of the beam section pattern detector



Fig. 29. 3-D figure of the beam section pattern detector

(6) Vacuum Leak Test Chamber in the Plasma Diagnostics Laboratory

Preliminary vacuum leak tests were carried out on several diagnostic devices to be used for the LHD plasma experiment with this chamber. For example, Thomson 4I flange, FIR ZnSe and BaF<sub>2</sub> windows, dispersion windows, reflectometer windows, visible camera windows, MIR

windows, penning H $\alpha$  and laser blow flanges, IR bolometer CaF<sub>2</sub> and ZnSe windows, RF spectrometer flanges etc.

We carefully tested the vacuum components. Therefore, in this 16th experimental campaign, the plasma experiment was not stopped because of the diagnostic device vacuum leakage.

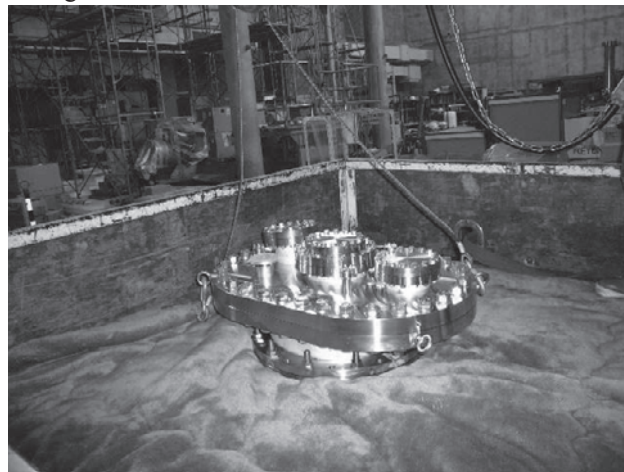


Fig. 30. Snap shot of the leak test for the Thomson 4I flange

(7) Development of Data Acquisition Systems

In the LHD data acquisition (DAQ) system, 7 new DAQ PCs have been added in 2012. One of them uses the new thermocouple input modules and the DAQ system has been modified to acquire the temperature measurement data by these new modules.

The other one has 38 high-voltage ADC modules (290 channels) in 3 PXI chassis, and it acquires 5MB data per channel for a short-pulse shot. It means this one DAQ PC acquires, stores and manages 1.45GB data per shot. Totally, the amount of the acquired data of the whole DAQ system increased to 17.4GB (7.5GB after compressed) per short-pulse shot and it recorded 328GB for one steady-state shot. In 2012, the total size of acquired data has reached 89TB.

The DAQ system stored this extremely huge amount of data to the cloud-based storage system "IznaStor" in the 16th campaign. But considering costs, we tested and evaluated the performance of the free software "GlusterFS" that is a scale-out NAS file system for the next campaign.

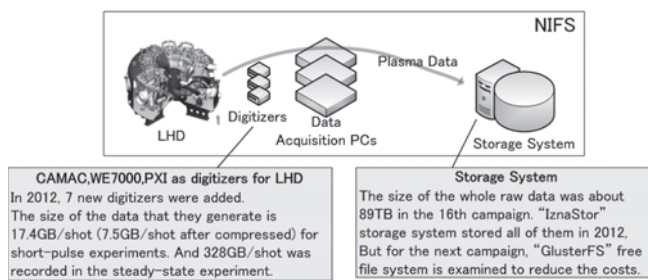


Fig. 31. Overview of the LHD Data Acquisition Systems for

the 16th experimental campaign

### 5. Control Technology Division

The Control Technology Division contributed to those important technological parts of the LHD, such as operation and management and development of the system. The work of the system operation and system management is as follows; operation of the cryogenic system and the power supply system for the super conducting coils, updating the central control system and cryogenic control system and coil quench detection system, and management of the network system. The work of the system development in this year is as follows; development of a new simulation algorithm for the cryogenic system, system development of the control system for LHD, and etc. Details of the activities in this division are described.

#### (1) Operation of LHD

LHD cryogenic system operation started on July 17 in the sixteenth-experimental campaign, the helium gas was purified as usual. The coil cool-down was started at August 1, but it was stopped because of the repair of a insulation pipe of the LHD poloidal coil. And then the LHD cryogenic system operation restarted on September 14, and the coil cool-down was completed on October 15. The number of steady-state operation days of the super conducting coils was 54 days. Although a failure of T2 turbine happened and the cryogenic system capacity decreased, it was able to operate safely without serious trouble. The coil warm-up was started on December 7, and it was finished on December 28. In the coil warm-up, a change was made changed to a new cryogenic control system, and it was proved that the new cryogenic control system could operate correctly. The availability of the cryogenic system achieved 95.7 %, and the total operation time was 3,742 hours in this campaign.

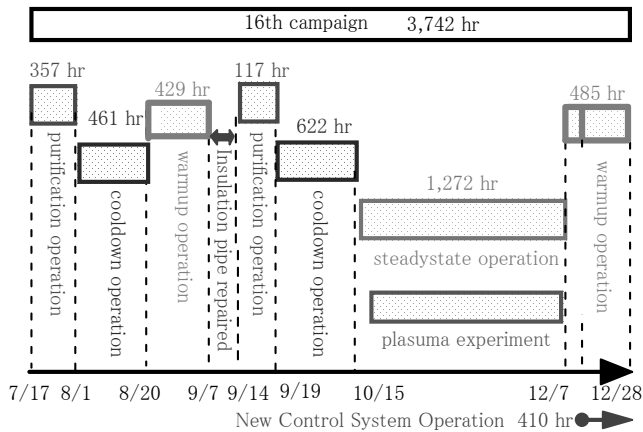


Fig. 32. Operation experience of LHD cryogenic system.

The first excitation of LHD in the sixteenth-experimental campaign was on October 15, and it was finished on December 6. The number of excitation times of LHD was 40 times, and total operation time was 342 hours in this campaign. In these operations, the high voltage power supply for pulsed excitation was used 2 times and the polarity switch device was used 14 times.

#### (2) Update of LHD Central Control System

The central control system requires high reliability. Since starting 17 years have passed; and it has become difficult to obtain maintenance parts. We decided to update these apparatuses over three year time. Five client PCs, servers and Programmable Logic Controller in the central control board were replaced with new ones last year. In this year when it was the second year, we updated the timing board, monitor system and backup server system.

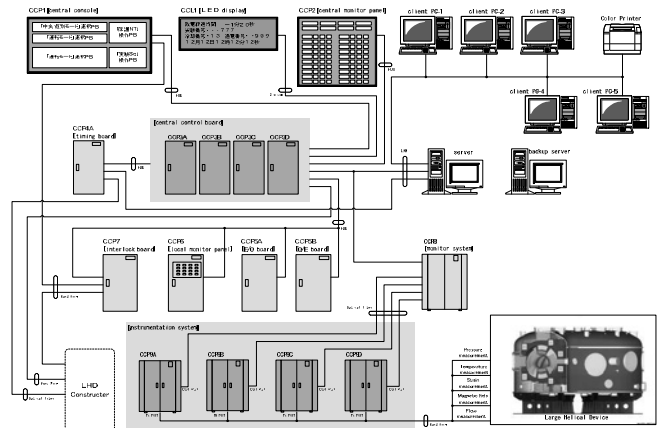


Fig. 33. Block diagram of central control system.

#### (3) Update of LHD Cryogenic Control System

Parallel running of a VME system and a CPCI system was performed during cooling and steady operation this year for the check of the system. The operation of the program was satisfactory. It changed from VME to CPCI in the middle of the warming operation in about 8 hours. It operated correctly carrying out thermal control for 18 days from the day following the transfer to normal temperature. The VME was separated after that and the CPCI full duplication work was done.

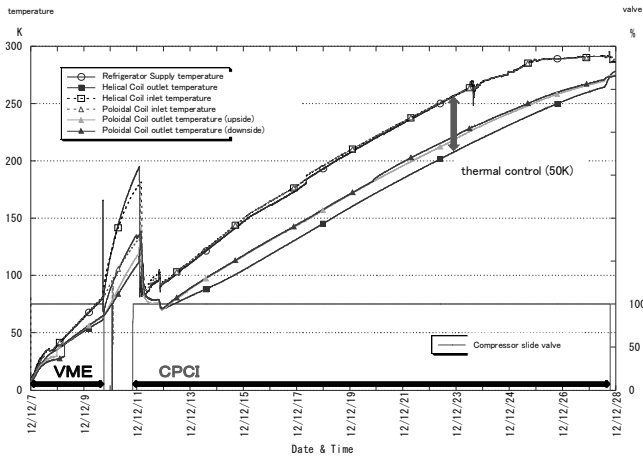


Fig. 34. Chart of LHD cryogenic system temperature during warm-up operation.

(4) Improvement of Helical Coil Quench Detector

The LHD superconducting helical coil uses a quench detector for protection. The 15th experiment was interrupted by a malfunction of the detector 6 times. But in the last year (16th experiment) as a result of investigation and improvement there was no malfunction. We report about this improvement.

Quench detector is made up of 3 blocks (comparator, timer and judgment circuit). As a result of the investigation we found a problem in the timer circuit. The response time of judgment circuit was about 200nsec (filter time constant) On the other hand the timer circuit consisted of a IC555 and the response time was about 100nsec, faster than the judgment circuit. The imbalance of the response time caused a malfunction occasionally.

We reconstructed the timer circuit that used a general timer relay (Fig. 35). The response time of the timer relay was 20msec ~ 100msec, slower than the judgment circuit. Therefore, it is difficult for the detector to malfunction. Before and after the improvement we checked by the mock pulse (Fig. 36). And we verified that the problem was solved (Fig. 37 Pulse waveform).

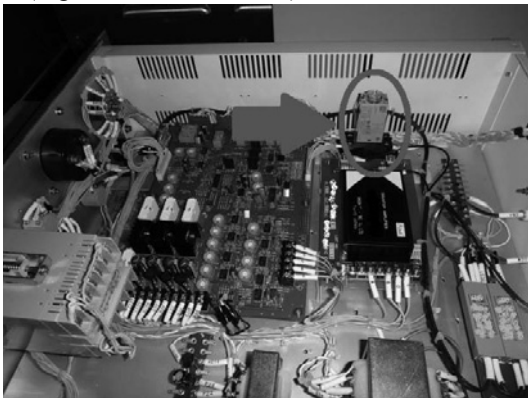


Fig. 35. Timer relay.



Fig. 36. Checking the system.

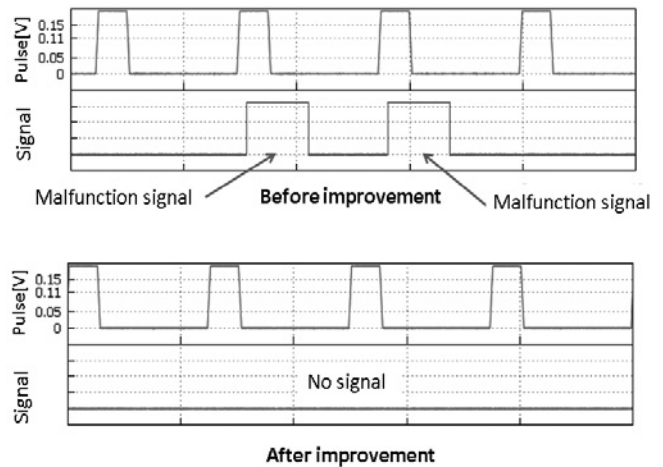


Fig. 37. Pulse waveform.

(5) Network management

The NIFS campus information networks consists of several clusters. We managed the Research Information Cluster (NIFS-LAN) and the LHD Experiment Cluster (LHD-LAN).

(5.1) NIFS-LAN

NIFS-LAN is the network of general use, and covers the whole campus region. We have administrated the Routers, layer-2 / layer-3 switches, Mail server, SSL-VPN server, DNS server and DHCP server.

New contributions in FY 2012 are as follows:

(a) Renew the core system

The NIFS-LAN core switch which had been installed in FY 2000 has been replaced with a Cisco Nexus 7009 layer-3 switch (Fig. 38). The virtual server system and the external connection switch also have been introduced simultaneously.

(b) Replace Wireless LAN Access Point

The wireless LAN access point has been replaced with a WZR-600DHP in order to further enhance the security and

convenience. This machine supports IEEE 802.11n/a/b/g. The security key which was pointed out to have a vulnerability was changed into WPA2 from WEP.

(c) Distribute the SEP version 12.1.2

We started to distribute the Symantec Endpoint Protection (SEP) version 12.1.1, which covers Windows8.

(d) Upgrade the operating system of the SSL-VPN server

The operating system of the SSL-VPN server was upgraded in order to make remote access service users available to the Windows8 and newer versions of security software.

(e) Development of an electric application system

An electronic application system was developed in order to reduce the approval time of the remote access continued use application.

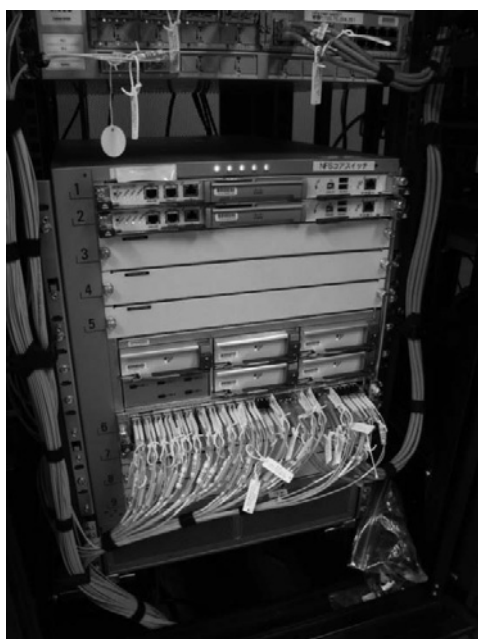


Fig. 38. The new NIFS-LAN core switch (Nexus 7009).

(5.2) LHD-LAN

The LHD-LAN has been contributing to the LHD experiments since 1996. The new “LHD-LAN Core Switch System” has been renewed in the 2007-2008 fiscal years. The main part consists of two Cisco Catalyst 4507R multi-layer switches connected by a 10 Gbps Ethernet, whose maximum throughput is over 210 million packets per second.

New contributions in FY 2012 are as follows:

(a) Renewal of the LHD Access gateway

We had operated the gateway device SA4000, which interconnected between the Research Information Cluster and the LHD Experimental Cluster. However support by the maker was finished. Therefore we replaced it with a MAG4610 made by the same company; Juniper Network

Inc.

It is possible that up to 5000 users access to the MAG4610 simultaneously. Also, MAG4610 is not a device for VPN communication unlike SA4000. MAG4610 dynamically asks the interlocking firewall (SSG550M) to give a passing allowance. As a result, communication speed became much higher. When devices were replaced, we organized user accounts. As a result, we could delete approximately 60 unused accounts. As for day to day business, we respond to user’s inquiries, update the security policy, and so on.

(b) Renewal of Firewall

We updated a firewall to SSG550M (Juniper company) which could link MAG4610. The performance is more than 1Gbps, and the number of the biggest simultaneous sessions is 256,000.

Fig. 39 is a photograph of MAG4610 and SSG550M.



Fig. 39. MAG4610 and SSG550M.

(6) Development of control systems using a FPGA embedded board

We have routinely received development requests about control systems from researchers, and carry out everything from consultation to implementation and maintenance. The requests are involved in a software/hardware renewal in aging control systems, modification of existing systems, development of new control systems and so on. Though the most popular requests are development of plant operation and monitoring systems, requests for feedback control systems and timing control systems, which require quick response from microseconds to milliseconds, are increasing in recent years. In these cases, we should use a dedicated embedded board, with FPGA and Linux OS on it, rather than a general-purpose controller like PLC because of the restriction of responsiveness.

However, in the development using an embedded board, it is necessary to customize software and hardware from the fundamental mechanisms to meet the required specifications, and it has been a factor to prolong the development period.

This fiscal year, we have developed a reusable middleware by standardizing the data transmission protocol between the FPGA and external nodes. It enables not only the reduction

of the development period drastically but also an easy setup and monitoring of the FPGA as in the case of using a PLC.

The middleware was adopted to the ECH injection synchronous system and its efficiency was proven in the 16<sup>th</sup> plasma experimental campaign.

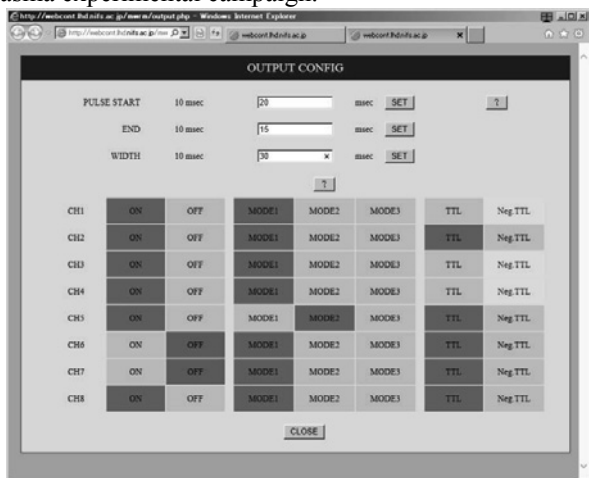


Fig. 40. ECH injection synchronous system.

(7) Validation of CEA test loop experiment to study ITER relevant supercritical helium loop

The dynamic simulation of the CEA (Commissariat an l'energie atomique et aux energies alternatives) test loop experiment to study the ITER relevant supercritical helium (SHe) loop was carried out.

The dynamic simulation system, C-PREST, has been utilized to study the thermal-hydraulic behavior of a forced-flow SHe loop. Fig. 41 shows a schematic of the CEA test loop experiment, which consist of two immersed heat exchangers in an LHe reservoir, a circulation pump (CP), three independent heated sections along the loop and bypass valves for flow distribution. We successfully validated the simulation model in C-PREST by the end of 2012. In 2013, the operation to the mitigate heat load to the LHe reservoir by control of a bypass valve or CP rotational speed of the CEA test loop was simulated. Fig. 42 shows the return mass flow rate of the LHe reservoir with a controlled bypass valve. The result of the simulation was in good agreement with the experimental result. In the future, we will implement the process study of ITER cryoplant, i.e. TF structure, TF coil, CS, etc.

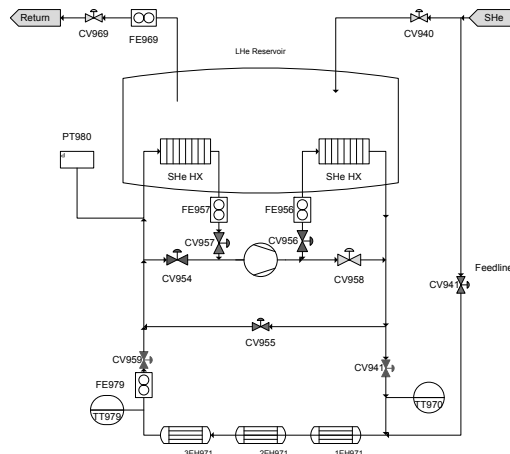


Fig. 41. Schematic of the CEA test loop experiment.

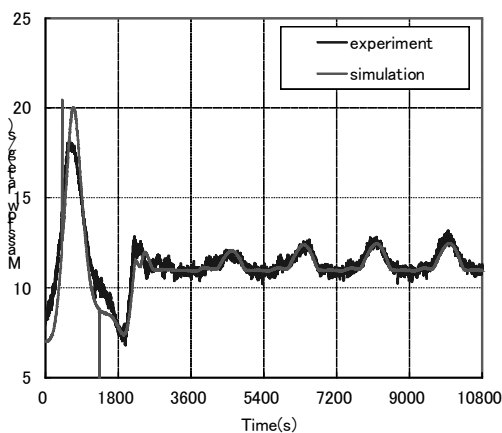


Fig. 42. Return mass flow rate of LHe reservoir.

6. Symposium on Technology, Technical Exchange and Dual System

(1) The Symposium on Technology

The Symposium on Technology was held on March 7 and 8, 2013 at Ehime University. There were 712 participants from many Japanese universities, national laboratories, technical colleges, and some industries.

In this symposium 375 papers were presented in 12 oral sessions and poster sessions. Technical experience and new techniques were reported and discussed. Nine papers were presented from our department.



Fig. 43. A snapshot of the poster session.

## (2) Technical Exchanges

The technical exchanges between our department and other institutes or universities were held in order to improve the technical skills of the staff. In this fiscal year, we invited Mr. Ohmine from November 26 to 30th. He is a technician belonging to Okinawa National College of Technology. He produced a small dynamometer housing as the teaching material for power measurement of the engine to use in his position. And the meeting “Symposium on Safety and Health Management in a Laboratory” was held on February 7 and 8, 2013 with 50 participants from 15 universities and 4 institutes.



Fig. 44. Training of a visitor.